Electronic Supplementary Material (ESI) for Physical Chemistry Chemical Physics.

Electronic Supplementary Information

Bismuth nanowires: electrochemical fabrication, structural features, and transport properties

Anna S. Goncharova[a], Kirill S. Napolskii[a,b*], Olga V. Skryabina[c,d], Vasily S. Stolyarov[c,d,e],
Eduard E. Levin[b,f], Sergey V. Egorov[c], Andrei A. Eliseev[a,b],
Yusif A. Kasumov[g], Valery V. Ryazanov[c,d], Galina A. Tsirlina [b,d]

[a]Department of Materials Science, M.V. Lomonosov Moscow State University,
119991, Moscow, Russian Federation
[b]Department of Chemistry, M.V. Lomonosov Moscow State University,
119991, Moscow, Russian Federation
[c]Institute of Solid State Physics, 142432, Chernogolovka, Russian Federation
[d]Moscow Institute of Physics and Technology, 141700, Dolgoprudny, Russian Federation
[e]Department of Fundamental Physical and Chemical Engineering, M.V. Lomonosov Moscow State University, 119991, Moscow, Russian Federation
[f]FSRC "Crystallography and Photonics" RAS, Leninskiy Prospekt 59, 119333, Moscow, Russian Federation
[g]Institute of Microelectronics Technology and High Purity Materials, 142432, Chernogolovka, Russian Federation

S1. Preparation of porous alumina templates

High purity aluminium foil (99.99%, 0.1 mm thick) was used as the starting material for the preparation of anodic aluminium oxide (AAO) templates. Prior to anodizing aluminium was cleaned with acetone and electrochemically polished in a solution containing of 185 g l^{-1} CrO_3 (>99.7%, Vecton, Russia) and 880 ml l^{-1} H_3PO_4 (85%, Chimmed, Russia) under anodic polarization at the current density of 0.4 A cm^{-2}. Then the Al plates were washed with deionized water and dried in air.

Al foils were anodized in two-electrode teflon electrochemical cell in 0.3 M $H_2C_2O_4$ (>99%, Chimmed, Russia) using Pt wire ring as a cathode. The electrolyte was rigorously stirred, and its temperature was kept in the range of 0–4 °C during anodizing.

In order to obtain templates with highly ordered porous structure and narrow pore size distribution, two-step anodizing of aluminium at constant voltage of 40 V was realized. The sacrificial layer formed during the first anodizing for 12 h was selectively etched away in a mixture of 35 ml l^{-1} H_3PO_4 and 20 g l^{-1} CrO_3 at 70 °C. After the second anodizing under the same conditions for 24 h the porous oxide layer of ~60 μm thicknesses was obtained.

To prepare AAO films possessing pore diameter of ~100 nm hard anodizing technique was applied. Anodizing voltage was increased to the target value of 120 V with a rate of 0.5 V s^{-1} and then was kept constant until charge density reached 100 – 200 C cm^{-2}, which is sufficient for the formation of 50 – 100 μm thick AAO. The porous templates obtained at 40 and 120 V are denoted as AAO_40V and AAO_120V, respectively.

To separate the oxide film from the substrate, remaining aluminium was dissolved in a solution containing 0.5 M $CuCl_2$ (98.5%, Chimmed, Russia) and 5 vol. % HCl (35-38%, IREA2000, Russia) at room temperature for 10 minutes. Subsequently, the pore bottoms were opened by chemical etching in a 5 vol. % H_3PO_4 water solution at 60 °C for 5 and 17 min for AAO_40V and AAO_120 V, respectively. According to SEM, pore diameter in through-pore AAO_40V and AAO_120V templates was 53 ± 5 nm and 100 ± 20 nm, respectively.

S2. Features of Bi electroplating electrolyte based on the mixture of water and ethylene glycol

The conductivity of electrolytes (red squares in Fig. S1A) was measured using standard Malvern Panalytical disposable capillary cell DTS1070 for Malvern Zetasizer Nano instrument. Bath pH (blue circles in Fig. S1A) was estimated using Expert-001 ionometer equipped with glass electrode. The measured values of pH have a meaning of glass electrode potential in the mixed solvent (the mixture of ethylene glycol and water with volume-to-volume ratio of 7:3). These values cannot be treated quantitatively in terms of hydronium ion activity because autoprotolysis constants of the mixture differ from that for pure water [1], and also because purely aqueous reference is used. In what follows we apply these apparent pH values only for comparative characterization of solutions acidity in one and the same mixed solvent.

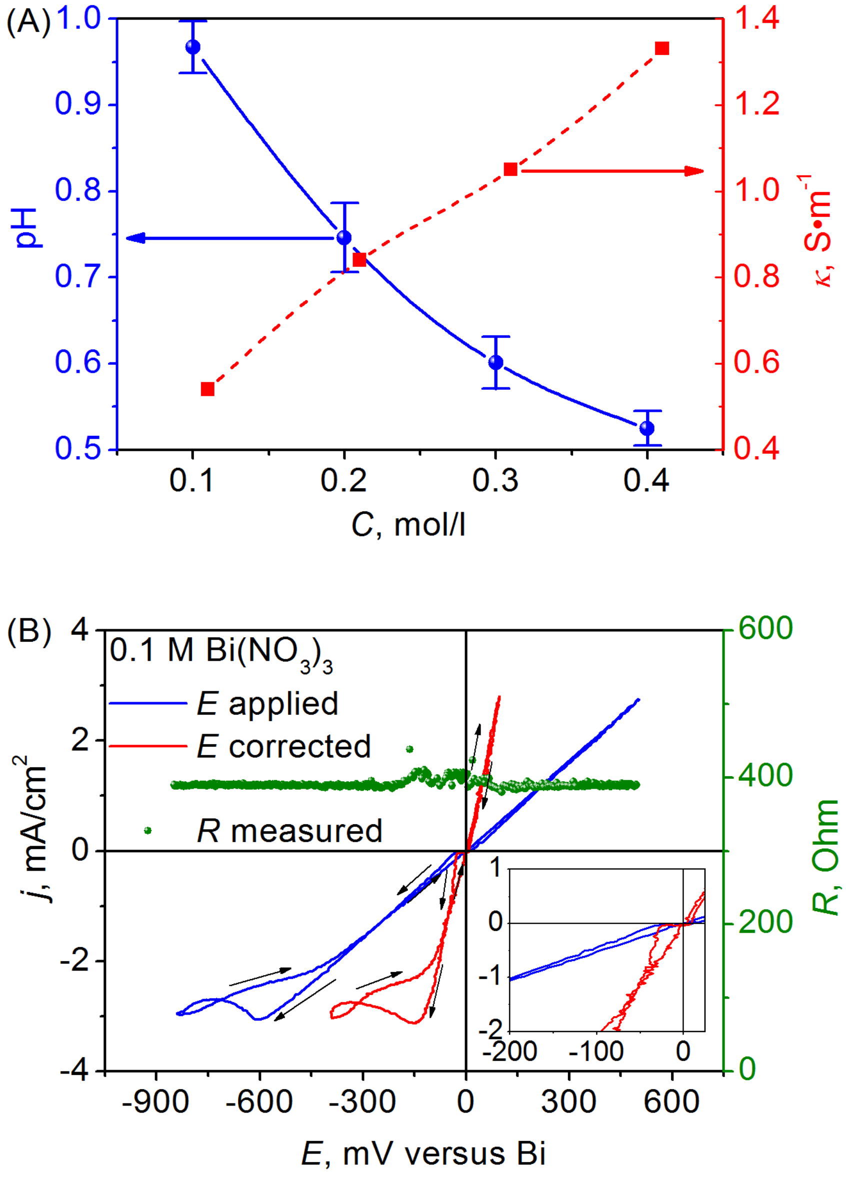

Fig. S1. (A) Dependence of pH (blue circles) and conductivity κ (red squares) of electrolyte aged for 1 month on concentration of Bi(NO$_3$)$_3$ in a solution. (B) Cyclic voltammetry data recorded in the bath containing 0.1 M Bi(NO$_3$)$_3$ on a bare polycrystalline Au plate with predeposited 2.5 µm thick Bi. Potentials are given versus Bi reference electrode. Cyclic voltammogram recorded without iR correction at potential scan rate of 5 mV s^{-1} is shown by blue curve. Green dots correspond to the resistance of electrolyte between working and reference electrodes (measured using current interrupt technique) versus applied potential difference. Cyclic voltammogram recalculated taking account of iR drop of potential is shown by red curve.

The complication we met for deposition of Bi from rather viscous electrolyte based on the mixture of water and ethylene glycol is the dependence of current density on the geometric surface area of working electrode. We compared the data for cells with 0.8 and 0.2 cm^2 surface area of working electrodes, and concluded that the difference in calculated current densities exceeds the inaccuracy of geometric area determination. The calculated current density is higher for working electrode with smaller geometrical surface area. Qualitatively this disagreement remained the same for the cells with various geometry of vessel near the bottom (cylindrical or conical), so it is hardly induced by the Ohmic drop of potential in used electrolyte. The larger electrode we use, the higher current passes through the cell and the higher Ohmic drop of deposition potential from setting value is observed. In what follows we compare only the data for electrodes with one and the same geometric surface area.

The measurement of Ohmic drop of potential within electrolyte was carried out using the current interrupt technique. Before each potentiostatic experiment, the electrolyte resistance was measured (Table S1) and then 95% of the obtained value was compensated.

Table S1. Ohmic resistance of electrolytes for Bi deposition measured by current interrupt approach.

Concentration of $Bi(NO_3)_3$ in electrolyte	Applied potential, V versus bulk Bi	Ohmic resistance, Ohm
0.1 M	−0.2	400 ± 10
0.2 M		268 ± 2
0.3 M		214 ± 2
0.4 M		190 ± 5

S3. Polarization behaviour in Bi-free electrolytes

Contribution of background processes was estimated using voltammetry in Bi(III)-free solutions (Fig. S2). To imitate the acidity of solutions used for Bi deposition, HNO_3 was added to the mixture of ethylene glycol and water taken in volume ratio of 7:3. The voltammograms were recorded in the interval −0.05 ÷ −1 V versus Ag/AgCl with a scan rate of 5 mV s^{-1}. To compare background processes for Au and Bi substrates, bulk polycrystalline Au electrodes with and without predeposited 2.5 μm thick Bi were used. For this purpose, Bi layer was formed from the bath containing 0.4 M $Bi(NO_3)_3$ at deposition potential $E_d = -0.2$ V. Before recording of cyclic voltammograms the electrolyte solution was deaerated by argon for 30 min. Then, to prevent penetration of oxygen into electrochemical cell, argon was blown above electrolyte during measurements.

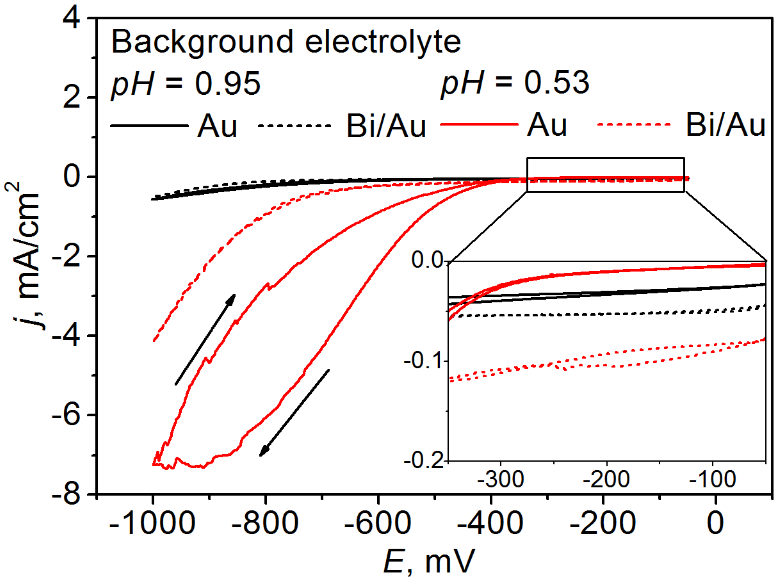

Fig. S2. Cyclic voltammograms recorded for Bi-free baths at potential scan rate of 5 mV s^{-1}. A bare polycrystalline Au plates with (marked as Bi/Au) and without predeposited Bi (marked as Au) served as working electrodes. Potentials are given versus saturated (KCl) Ag/AgCl reference electrode.

Table S2. Content of Bi in electrodeposited specimens according to ICP mass-spectrometry analysis.

Concentration of $Bi(NO_3)_3$ in electrolyte	**Deposition potential, V vs bulk Bi**	**Bi content in electrodeposited specimens, wt. %**
0.1 M	−0.1	99.2±2.8
	−0.2	98.9±2.8
0.4 M	−0.1	99.2±2.8
	−0.2	99.3±3.2

S4. Morphology of bismuth deposits on bare substrates

	-0.2 V	-0.9 V
0.1 M	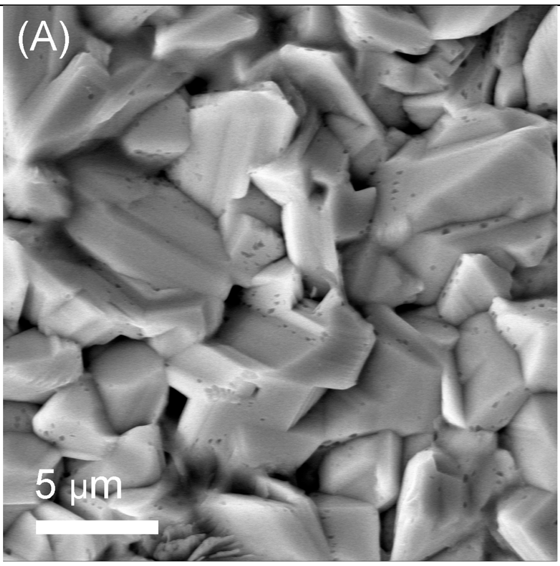	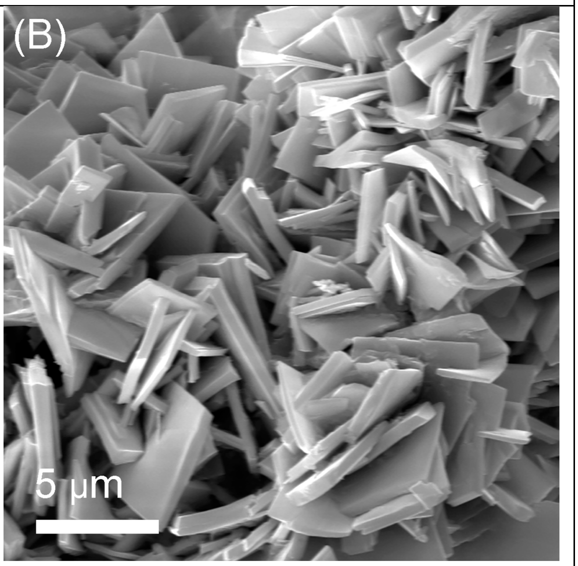
0.4 M	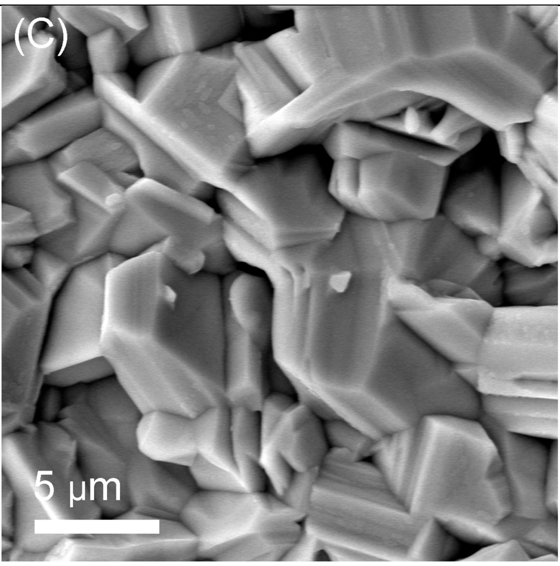	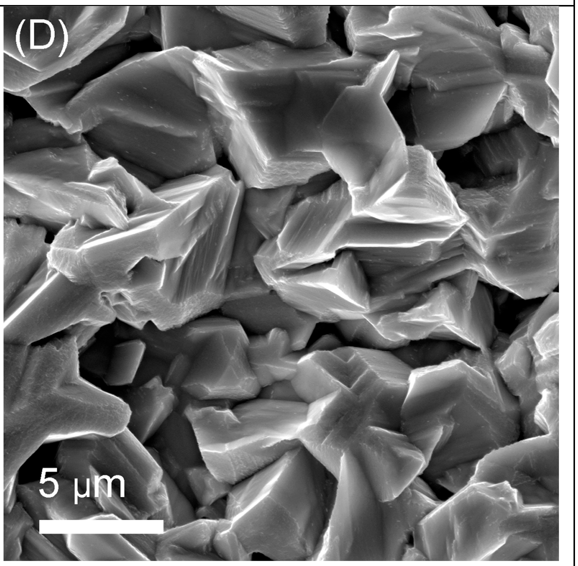

Fig. S3. SEM images of Bi deposits obtained in kinetic (left column) and diffusion (right column) regimes on bare Au/Bi substrates. Electrolytes containing 0.1 M and 0.4 M $Bi(NO_3)_3$ were used.

S5. Long-term stability of Bi nanowires in suspended form

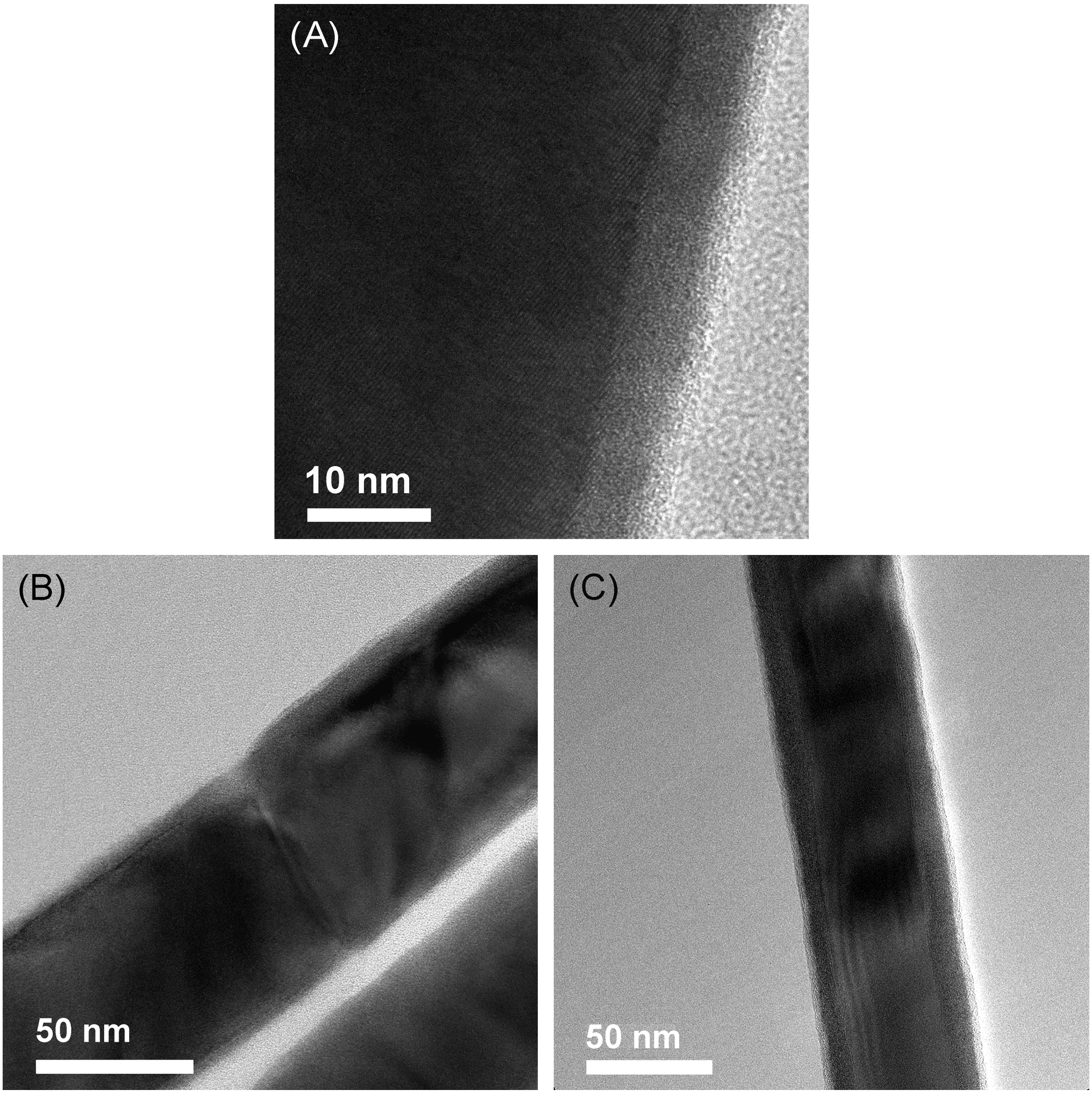

Fig. S4. (A) HRTEM data for as-prepared Bi nanowire obtained from the electrolyte containing 0.4 M $Bi(NO_3)_3$ at $E_d = -0.2$ V. TEM images of bismuth nanowires suspended in hexane (an aprotic solvent): (B) as-prepared, (C) after one month storage.

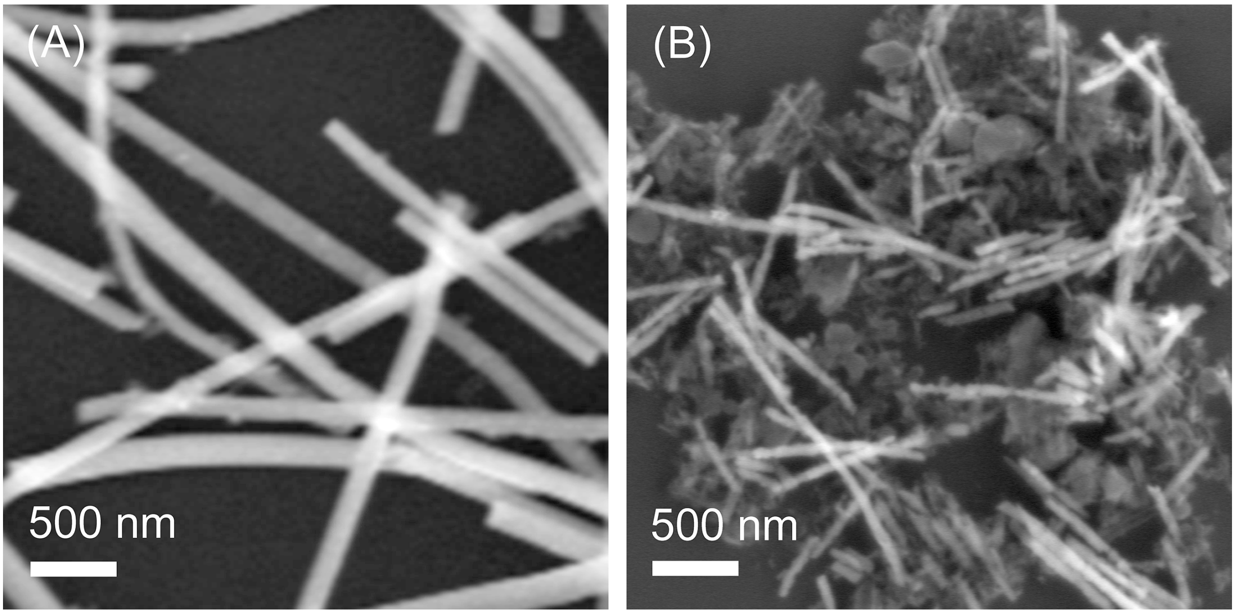

Fig S5. SEM images of Bi nanowires seeded onto Si/SiO$_2$ substrates from (A) as-prepared and (B) four month aged isopropanol-based suspensions. Nanowires are obtained from the nanocomposites based on AAO_120V (A) and AAO_40V (B).

S6. Transport measurements of individual Bi nanowires

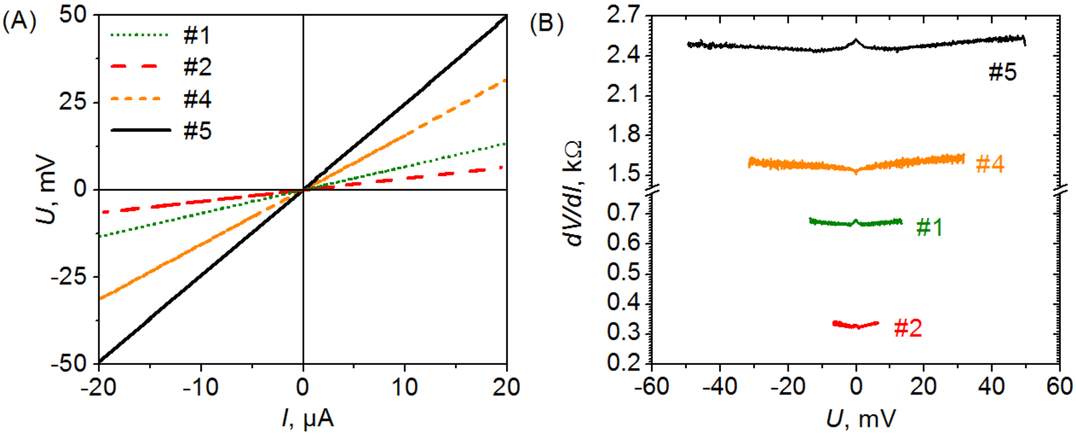

Fig. S6. $V(I)$ (A) and $dV/dI(V)$ (B) curves for single Bi nanowires measured at 1.2 K. Data for the samples #1, #2, #4, and #5 are presented by green, red, orange, and black lines, respectively.

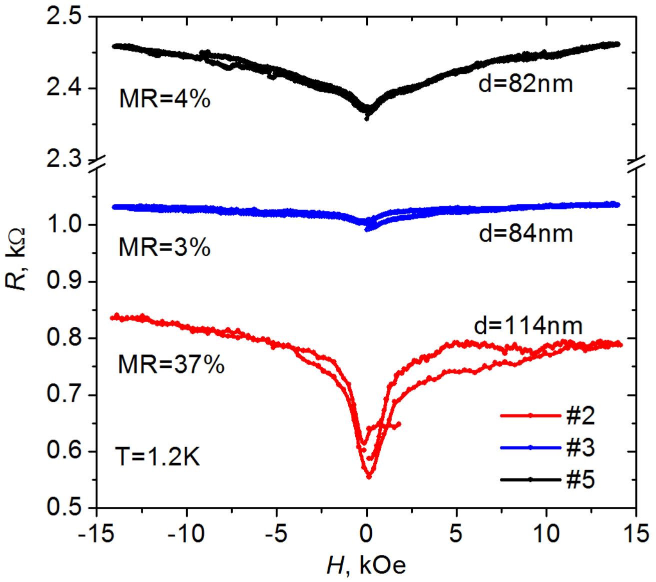

Fig. S7. Typical dependence of the resistance on the perpendicular magnetic field at 1.2 K for individual Bi nanowires. Data for the samples #2, #3, and #5 are presented by red, blue, and black lines, respectively. The current of 50 nA has been passed through the samples during measurements.

References

[1] S. Rondinini, P.R. Mussini, T. Mussini, and A. Vertova, pH measurements in non-aqueous and mixed solvents: Predicting pH(PS) of potassium hydrogen phthalate for alcoholwater mixtures (Technical Report), *Pure and Applied Chemistry,* (1998) pp. 1419-1422.